Evaluation of mechanical strength and durability characteristics of eco-friendly mortar with cementitious additives

Trong-Phuoc Huynh[1,*], Dinh-Thang Nguyen[2], Thanh-Duy Phan[3], Nguyen-Trong Ho[4], Phuong-Trinh Bui[5,6], and May Huu Nguyen[7,8]

[1] *Department of Civil Engineering, College of Engineering Technology, Can Tho University, Campus II, 3/2 St., Ninh Kieu Dist., Can Tho City 900000, Vietnam*
[2] *School of Graduate, Can Tho University, Campus II, 3/2 St., Ninh Kieu Dist., Can Tho City 900000, Vietnam*
[3] *Department of Civil Engineering, Faculty of Engineering at Kamphaeng Saen, Kasetsart University, Malaiman Rd., Kamphaeng Saen Dist., Nakhon Pathom City 73140, Thailand*
[4] *Faculty of Civil Engineering, VSB – Technical University of Ostrava, Ludvíka Podéště 1875/17, 708 00 Ostrava-Poruba, Czech Republic*
[5] *Department of Construction Materials, Faculty of Civil Engineering, Ho Chi Minh City University of Technology (HCMUT), 268 Ly Thuong Kiet Street, District 10, Ho Chi Minh City, Vietnam*
[6] *Vietnam National University Ho Chi Minh City, Linh Trung Ward, Thu Duc District, Ho Chi Minh City, Vietnam*
[7] *Civil and Environmental Engineering Program, Graduate School of Advanced Science and Engineering, Hiroshima University, 1-4-1, Kagamiyama, Higashi-Hiroshima, Hiroshima 739-8527, Japan*
[8] *Department of Bridge and Tunnel, Faculty of Civil Engineering, University of Transport Technology, 54 Trieu Khuc, Thanh Xuan, Hanoi 100000, Vietnam*
[*] *Corresponding author. E-mail: htphuoc@ctu.edu.vn*

Received: Nov. 04, 2020 Accepted: Mar. 11, 2021

The mechanical strength and durability of eco-friendly mortars used in the repair of marine concrete structures exposed to freshwater and seawater environments were evaluated in this paper. The eco-friendly mortar samples were produced using various ratios of fly ash (FA), ground granulated blast-furnace slag (GGBFS), and silica fume (SF) as cementitious materials. Seven mixtures of eco-friendly mortars, including a control mixture; three mixtures with respective substitutions of GGBFS for Portland cement of 10, 20, and 30% by cement mass; and three mixtures with respective additions of SF of 5, 10, and 15% by total binder mass, were used to produce the samples. Tests, including compressive strength, flexural strength, ultrasonic pulse velocity (UPV), electrical surface resistivity (ESR), rapid chloride ion penetration (RCP), thermal conductivity (TC), and microstructure analysis, were conducted to determine the mechanical strength and durability values of the samples. The experimental results show that replacing Portland cement with GGBFS negatively affected the properties of the mortars by reducing the mechanical strength, UPV, ESR, and TC while increasing the RCP in the samples. Also, adding an appropriate amount of SF could improve the mechanical strength and durability characteristics of the eco-friendly mortars. As a result, the mortar sample containing 30% GGBFS and 10% SF earned compressive and flexural strength values of approximately 49.2 and 13.8 MPa, respectively, at 56 days of curing age. Mortar samples with UPV values >3660 m/s were identified as "high quality". The corrosion resistance of all of the samples was found to be high, particularly in chloride-contaminated environments, due to relatively low (1000 - 2000 Coulombs) RCP values. The best overall performance was recorded for the sample containing 30% GGBFS and 10% SF.

Keywords: Eco-friendly mortar; Rapid chloride-ion penetration; Ultrasonic pulse velocity; Thermal conductivity; Electrical surface resistivity

http://dx.doi.org/10.6180/jase.202108_24(4).0010

1. Introduction

Hydraulic structures are widely used in water conservancy infrastructure projects [1–3]. Over their service life, aggressive agents in the marine environment constantly ingress into these structures, promoting severe deterioration over time [3–5]. Thus, using appropriately durable materials is widely recognized as crucial when building hydraulic structures and an important area of focus for researchers [1, 6, 7]. Mortar has gained increasing attention recently as an approachable solution to improve the problem of deterioration in offshore concrete structures [8–11].

Although many types of mortar are currently used in the repair and maintenance of offshore concrete structures, sufficient scientific evidence regarding their respective efficacies is lacking [8]. A series of scientific tests on eco-friendly mortar made from industrial wastes such as fly ash, slag, and silica fume has been conducted to obtain mortars with engineering properties that are superior to conventional mortars [12, 13]. In a study of the effect of secondary copper slag as a cementitious material on ultra-high performance mortars [9], it was found that the mortar containing copper slag exhibited increased flow and reduced compressive strength compared to the mortar containing no copper slag due to the copper slag reducing cement hydration and hardening time. Wang et al investigated the effect of fly ash on the properties and microstructure of repair mortar produced using a ratio of alkali-activated fly ash/blast furnace slag (FA/BFS) [10]. They found that the mechanical strength of the repair mortar produced from the FA/BFS ratio was highly dependent on the content of amorphous phases because the amorphous phases facilitated the degree of the polymerization reaction and the formation of the product. Moreover, although the particle-size distribution of fly ash did not affect the mechanical strength, obvious effects on the yield and shrinkage values of the mortar sample were observed. In addition, mortar made from an alkaline-activated FA/BFS mixture revealed high adhesion strength that made it suitable for use in concrete repair. The physico-mechanical properties of secondary mortar utilizing alkali-activated binary mortar (AABM) with 70 by wt.% volcanic pozzolana and 30 by wt.% ground granulated blast-furnace slag (GGBFS) were also previously investigated [11], with results indicating that compressive and tensile strengths at 28 days of curing were 34.8 MPa and 2.13 MPa, respectively. Moreover, the capillary absorption coefficient and modulus of elasticity were 0.5008 $kg/m^2h^{0.5}$ and 8.55 GPa, respectively, and the pull-off adherences of the C25/30, C35/45, and C50/60 concrete types were 0.75, 1.14, and 1.24 MPa, respectively. Thus, the quality of concrete promotes the adherent nature of the AABM. Based on the study of Robayo-Salazar et al. [11] and the standard specification of BS EN 1504-3:2005 (2005), AABM material may be classified as an R2-type repair mortar.

A new, free-cement binder that incorporates a ternary binder has been recently proposed for the production of eco-friendly mortar [14, 15]. In line with this development, several binders incorporating GGBFS, rice husk ash (RHA), FA have been produced using different RHA/GGBFS weight ratios and three different amounts of FA as the activator. The compressive strength, water absorption and porosity, ultrasonic pulse velocity (UPV), electrical surface resistivity (ESR), and sulfate resistance of the proposed mortars were then assessed, with results showing that the proposed binders meet the standard for mechanical durability. In addition, using silica fume (SF) and other pozzolanic materials, including GGBFS and FA, to enhance binders has been shown to be one of the most efficient and economical solutions for producing high-performance, highly durable construction materials [16]. SF, comprised primarily of free silica, has a large specific surface area, making it highly reactive with the hydrates in cement. GGBFS may be used to partially replace cement to improve the mechanical properties of the final products. However, the reactivity of GGBFS is significantly less than SF [16]. In addition, replacing traditional Portland cement with the abovementioned cementitious materials has been reported to have environmental and economic benefits as well as to produce durable construction materials for sustainable development [17].

In this study, the authors extend their previous studies [14, 15] to propose eco-friendly mortars that use industrial wastes that are available both locally and abundantly as cementitious sources (i.e., FA, GGBFS, and SF) for the repair of marine concrete structures that are regularly exposed to freshwater and seawater environments. Seven mixtures of eco-friendly mortars, including a control mixture; three mixtures with respective substitutions of GGBFS for Portland cement of 10, 20, and 30% by cement mass; and three mixtures with respective additions of SF of 5, 10, and 15% by total binder mass, were used to produce the samples. All of the samples were tested for compressive strength, flexural strength, UPV, ESR, rapid chloride ion penetration (RCP), thermal conductivity (TC), and their microstructures were analyzed to determine the mechanical strength and durability characteristics of each.

2. Materials and mix proportions

2.1. Materials

The chemical compositions of the supplementary cementitious materials (SCMs) used in this research, including grade-40 Portland cement (PC40), GGBFS, FA, and silica fume (SF), are presented in Table 1.

As shown in Table 1, the CaO content of the FA was only 1.07%, which is significantly smaller than the value of 10% proposed for FA under TCVN 10302:2014 (2014) [18]. Thus, the fly ash used in this study was classified as acid ash (class-F). In addition, the total combined content of CaO, SiO_2, and Al_2O_3 in GGBFS and SF were 87% and 97.86%, respectively, which are both higher than the 70% required under ASTM C618 (2019) [19]. Thus, these two materials met the chemical properties required for use as cement replacements in this study. In addition, the high percentage of SiO_2 (97.54%) in the SF used in this study is expected to promote strength development and durability in the mortar due to the formation of calcium-silicate-hydrate (C-S-H) and calcium-aluminate-silicate-hydrate (C-A-S-H) gels [20, 21].

The grain size distribution of the PC40 cement, GGBFS, FA, and SF used in this study are shown in Fig. 1. As shown, the diameters of most materials were mostly less than 10 μm. Also, the sizes of the GGBFS and FA particles were almost the same, and were smaller than the sizes of the other materials.

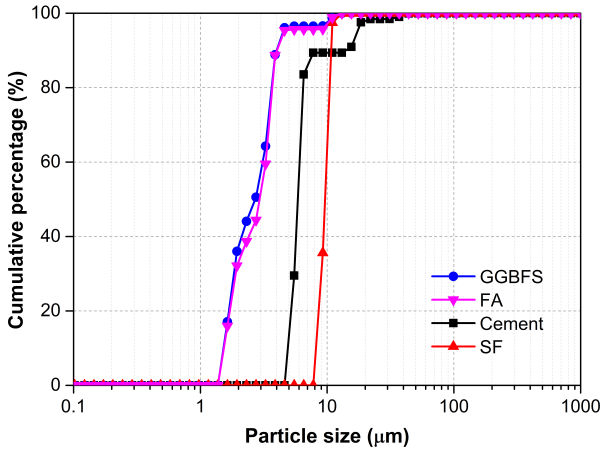

Fig. 1. Grain size distributions of the cementitious materials.

The morphologies of the raw materials, including PC40 cement, GGBFS, FA, and SF, are shown under scanning electron microscopic (SEM) in Fig. 2. The cement and GGBFS are shown to have irregular shapes, while FA and SF are comprised of a variety of spherical particles of differing sizes.

The mineralogical compositions of cement, GGBFS, FA, and SF were determined using X-ray diffraction (XRD), as shown in Fig. 3. The non-crystalline phase existed in the GGBFS and SF structures without a peak, while a high intensity of quartz was found in cement and FA, which is considered as the crystalize phase.

The fine aggregate used in this study was crushed sand with a density, water absorption, and fineness modulus of 2803 kg/m^3, 3.7%, and 3.0, respectively. In addition, a type-G superplasticizer (SP) was used to obtain the target workability of the fresh mortar mixture.

2.2. Mix proportions

The seven mixture proportions of the eco-friendly marine mortar used in this study are shown in Table 2. To investigate the respective influence of GGBFS and SF on the properties of eco-friendly marine mortar, six mixtures were used with differing ratios of GGBFS (10% [S10SF00], 20% [S20SF00], and 30% [S30SF00]) and SF (5% [S30SF05], 10% [S30SF10], 15% [S30SF15]) by mass. A standard mixture without GGBFS and SF (S00SF00) was also designed as the reference sample to compare and contrast the features of the proposed eco-friendly mortars.

The mortar mixtures were designed using a constant water-to-binder ratio of 0.39. Moreover, a suitable amount of SP was added to maintain the slump flow of the fresh mortar at 200 ± 5 mm. The properties of the marine mortar were evaluated based on the percentage of cement replacement by GGBFS and the amount of SF added to the mixture containing 30% SF (S30SF00).

3. Sample preparation and test methods

All of the raw materials were mixed in a laboratory mixer to ensure homogeneity. The process of mortar mixing and manufacturing was done in accordance with TCVN 3121-2:2003 [22]. The engineering properties of the hardened samples, including compressive and flexural strengths, UPV, ESR, RCP, TC, and microstructure, were tested up to 56 days of curing age. Tests of compressive and flexural strengths were conducted in accordance with ASTM C109 and TCVN 3121-11:2003, respectively [23, 24]. As required under ASTM C597, UPV was determined by using the rate of propagation of longitudinal and vertical stress waves to indicate the presence of voids and cracks [25], while RCP was determined in accordance with ASTM C1202 [26]. For the microstructure analysis, small pieces that had fractured after the compressive strength test were used for SEM observation in accordance with the procedures described in

Table 1. Chemical compositions of cementitious materials (% by mass).

SCMs	SiO_2	Al_2O_3	Fe_2O_3	MgO	CaO	Others
Cement	23.49	6.01	3.65	1.98	59.89	4.98
GGBFS	35.88	12.99	0.32	7.99	38.13	4.69
FA	59.17	26.71	6.06	0.89	1.07	6.10
SF	97.54	0.13	0.17	0.15	0.19	1.82

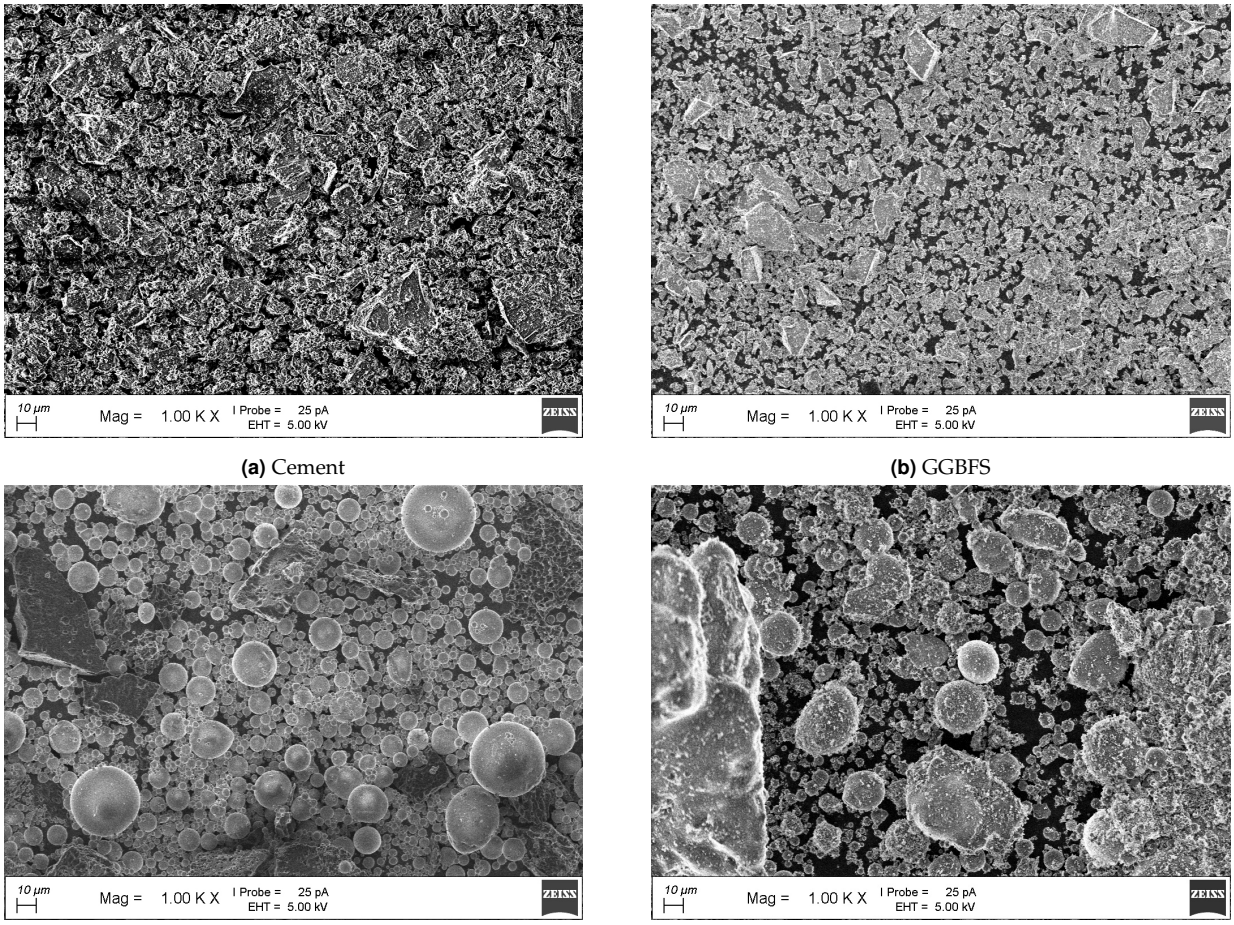

(a) Cement **(b)** GGBFS

(c) FA **(d)** SF

Fig. 2. SEM morphologies of the cementitious materials.

Table 2. Material proportions for each m^3 of mortar mixture.

Sample ID.	Materials (unit: kg)						
	Cement	GGBFS	FA	SF	Sand	Water	SP
S00SF00	413	-	136	-	1486	270	5.0
S10SF00	372	41	136	-	1485	270	4.7
S20SF00	330	82	136	-	1483	269	4.4
S30SF00	288	124	136	-	1482	269	4.1
S30SF05	282	121	133	27	1448	273	5.2
S30SF10	276	118	130	52	1416	277	6.6
S30SF15	269	115	127	77	1384	281	7.9

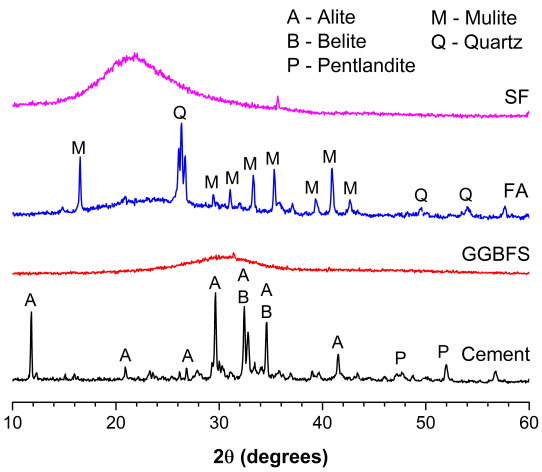

Fig. 3. XRD analysis of the cementitious materials.

Huynh et al. [14].

The ESR test was determined using the four-point Wenner array described by Kessler et al. [27]. Three cylindrical specimens with a diameter of 100 and a height of 200 mm were prepared and tested at 1, 7, 14, 28, and 56 days of curing age, respectively. A portable device (ISOMET 2104) was used to measure the TC of the cylindrical specimens under saturated-surface dry (SSD) and oven-dry (OD) conditions at 56 days of curing age [28].

4. Discussion of results

4.1. Compressive strength

The influence of GGBFS and SF on the development of compressive strength in the samples is shown in Fig. 4. As shown in Fig. 4a, compressive strength declines as GGBFS content increases. This may be explained by the higher Al_2O_3 content in GGBFS (12.99%) than in cement (6.01%; Table 1). Thus, active Al elements replace Si in the C-S-H gel to form C-A-S-H gel, which increases compressive strength in the slag-containing samples at later ages [29].

The influence of SF on the development of compressive strength, reflected in three main phases, is shown in Fig. 4b. In the first phase, on the first day of curing, S30SF05 had the highest compressive strength, and S30SF00, with the lowest amount of SF, had the lowest compressive strength. In the second phase (7 - 20 days of curing age), the highest-to-lowest ranking for compressive strength was S30SF10 > S30SF05 > S30SF15 > S30SF00. In the third phase (28 days of curing age), this ranking was S30SF10 > S30SF00 > S30SF05 > S30SF15. In phase one, SF exhibited higher pozzolanic reactivity and micro-fill effect, allowing an amount of SiO_2 in the SF to react with CaO in the cement and GGBFS to create C-S-H gel [30, 31], which strengthened the compressive strength of mortar samples at one day of curing age by a factor of 2 (S30SF00 vs S30SF10 or S30SF15) to 2.5 (S30SF00 vs S30SF05). In addition, unreacted SF particles may have remained in the mixture with high SF contents, leading to an incomplete pozzolanic reaction, which led to the trends observed in phases two and three. The hydration reaction created an amount of $Ca(OH)_2$ that enabled SF to participate in the secondary pozzolanic reaction and to continue creating C-S-H gel, which may explain the trend, observed in phase two, toward higher compressive strength due to greater bonding strength between the aggregate and mortar [32]. The third phase was influenced primarily by GGBFS because of the increase in pozzolanic reactivity caused by a large amount of generated $Ca(OH)_2$, which provided a favorable environment for the SiO_2 in SF to participate in the pozzolanic reaction.

In general, an excess amount of SF was found to reduce compressive strength significantly due to the high amount of fine particles in the SF increasing the surface area [33]. Therefore, 10% SF was determined in this study to be a reasonable replacement ratio to promote compressive strength development in mortar samples.

4.2. Flexural strength

The influence of GGBFS and SF on the flexural compressive strength of the samples at 7, 28, and 56 days of curing age, respectively, is shown in Fig. 5. Similar to the results for compressive strength, the highest flexural strength was obtained for the non-slag mortar sample (S00SF00) at all tested ages, with the significant 10 - 25% difference in flexural strength between S00SF00 and the others (S10SF00, S20SF00, and S30SF00; Fig. 5a) indicating that the presence of GGBFS slows the pozzolanic reaction. The flexural strength of the mortar samples tended to decrease as the amount of GGBFS increased. Notably, the difference in flexural strength between S20SF00 and S30SF00 was small, with a value range of 0.5 – 2.0 MPa. Therefore, S30SF00 was chosen as the control mixture for comparing the effect of adding SF on the engineering properties of eco-friendly marine mortar.

The influence of SF on the flexural strength of the mortar samples is shown in Fig. 5b. The flexural strength of S30SF10 was significantly higher than that of the other samples, with the ranking of flexural strength, from highest to lowest, as follows: S30SF10 > S30SF05 > S30SF15 > S30SF00. The presence of SF improved compressive and flexural strengths due to its filler effect and pozzolanic reactivity [34–36]. Numerous studies have shown that SF more positively influences flexural strength than compressive strength [35, 37, 38]. The optimal amount of SF as a cement

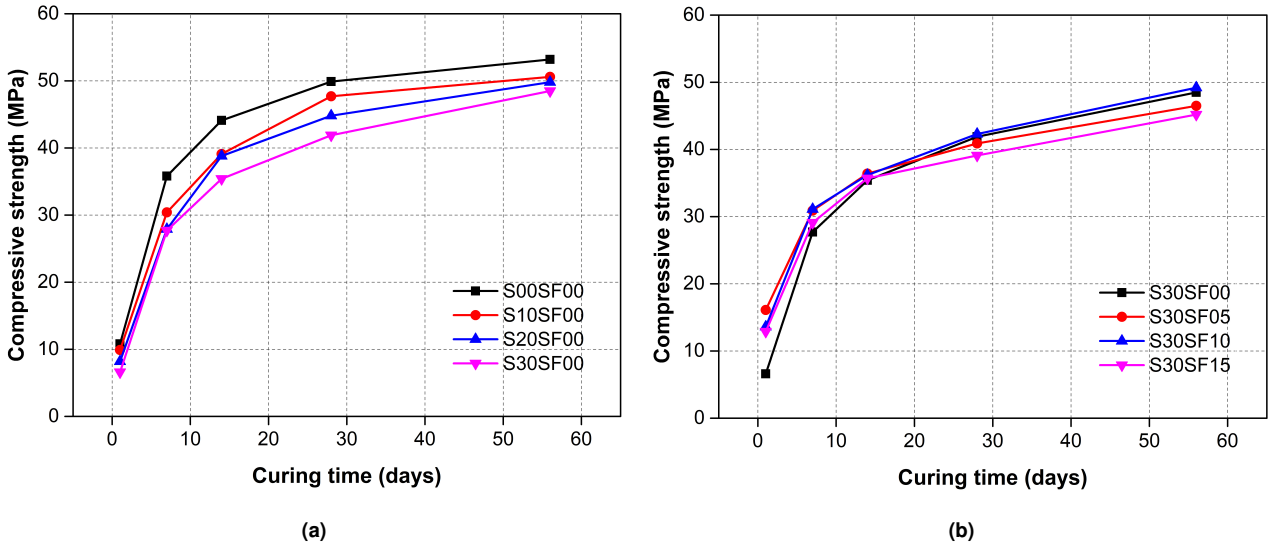

Fig. 4. Compressive strength development in eco-friendly mortar samples with various (a) GGBFS and (b) SF contents.

replacement ranges from 7.5 – 10% [39, 40], and 10% SF replacement is widely used [31] to improve flexural strength.

4.3. Ultrasonic pulse velocity

The influence of GGBFS and SF on the UPV of the eco-friendly mortar samples in this study is shown in Fig. 6. The 56-day UPV of the samples followed a pattern similar to the 56-day gain in strength discussed in previous sections, in which higher GGBFS replacement levels reduced UPV due to the slower pozzolanic reaction rate of GGBFS compared to the hydration of cement [41], and the use of 10% SF slightly increased the UPV measurements in the mortar samples. As mentioned previously, using an appropriate level of SF content (assumed at 10% in this study) was found to enhance the microstructure of the mortars (as observed in Fig. 12c) due to its filler effect and pozzolanic reactivity [31, 34, 37]. As a result, the denser internal structure of the mortars resulted in a higher UPV value. In this study, the UPV values of the eco-friendly mortar samples were in the ranges of 4038 – 4158 m/s, which were higher than 3660 m/s. Therefore, these samples were classified as high-quality mortars based on the proposal of Malhotra [42].

The relationship between UPV and compressive strength at 56 days of curing age for all of the mixtures is presented in Fig. 7. The obtained, approximate linear line was validated using a high coefficient of determination (R^2= 0.98), validating the close correlation between UPV and compressive strength in all of the mixtures, which concurs with the findings of previous studies [28, 43]. This result suggests that one of the two characteristics (UPV and compressive strength) may be used to determine the value of the other (see Fig. 7).

4.4. Electrical surface resistivity

As shown in Fig. 8, increasing the amount of GGBFS reduced ESR in the samples, with S00SF00, S10SF00, S20SF00, and S30SF00 earning ESR values of 54.1, 47.4, 42.5, and 35.6 kΩ.cm, respectively. Azarsa and Gupta [44] reported that the electrical resistivity of materials is greatly dependent on microstructural properties such as pore size and the shape of interconnections. In this study, the incorporation of GGBFS as a cement replacement resulted in a looser microstructure, especially at higher replacement levels (see Fig. 11), due to the slow pozzolanic reaction of GGBFS. Thus, fewer hydration products were generated, which was associated with a higher volume of voids/pores within the system and, subsequently, a lower ESR value. Similarly, for samples with various levels of SF, the ESR values were slightly reduced from 35.6 kΩ.cm (standard sample – S30SF00) to 33.2 kΩ.cm (S30SF05) and 32.2 kΩ.cm (S30SF30). However, the ESR value of 35.7 kΩ.cm for S30SF10 was slightly higher than that of the standard sample. Thus, the mixture with 10% SF replacement demonstrated adequate reliability in terms of ESR, as its microstructure was denser than the others (Fig. 12c). The ESR values of all of the eco-friendly mortar samples were >20 kΩ.cm, indicating a low rate of corrosion [45]. This result was in good agreement with the previously discussed patterns of development for strength and UPV in the samples (Sections 4.1 and 4.3).

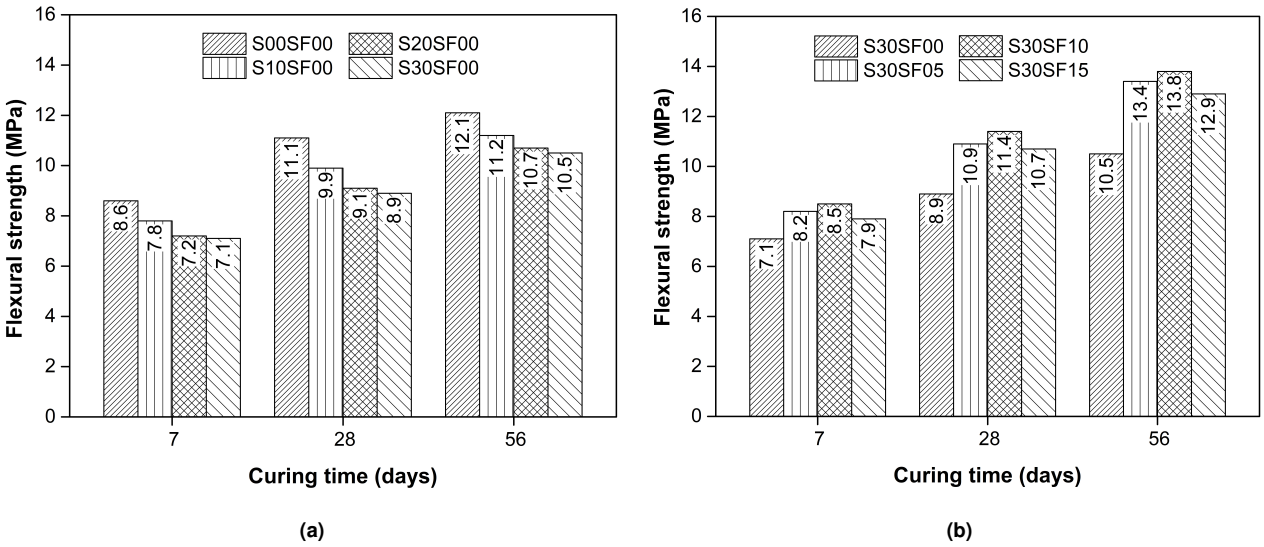

Fig. 5. Flexural strength development in eco-friendly mortar samples with various (a) GGBFS and (b) SF contents.

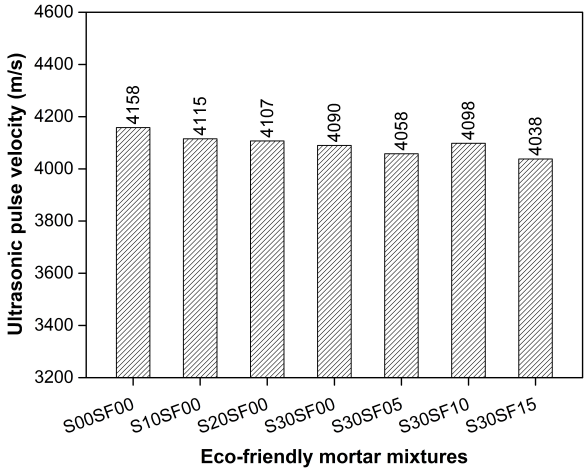

Fig. 6. UPV of the eco-friendly mortar samples.

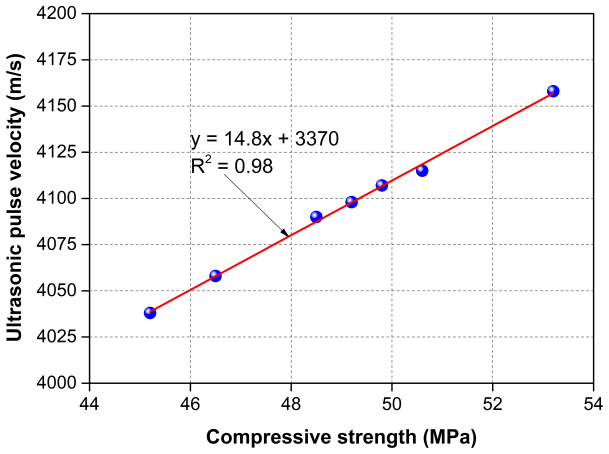

Fig. 7. The relationship between UPV and compressive strength in the 56-day-old mortar samples.

4.5. Rapid chloride-ion penetration

The RCP of the eco-friendly mortar samples was evaluated in this study by measuring the total amount of electrical current that passed through each sample, with the results shown in Fig. 9. The total charge transferred through the mortar samples was positively associated with the level of GGBFS replacement in the mortar mixtures. This was attributed to the reduction in microstructure density observed in Fig. 11. In addition, the mortar samples containing 10% SF exhibited better chloride permeability resistance than the mortar samples with 0%, 5%, and 15% SF. This result suggests an optimal content of 10% SF in the eco-friendly mortar mixture, where the chemical reactions were enhanced in chemically reactive environments. This finding is in line with results reported by other researchers [39, 40]. Thus, more hydration products were introduced into the system, which further densified the microstructure of the mortar samples (Fig. 12c) and led to lower RCP values. The total charge passed ranged between 1058 and 1922 Coulombs, which falls within the range allowed under ASTM C1202 [46]. The low RCP values of the samples support their good corrosion resistance, especially in chloride-contaminated environments. The high resistance to chloride penetration was attributed mainly to the increase in tortuosity in the pores of the mortar sample because of the presence of aggregates. In particular, the lowest ion penetration was reported for S30SF10, demon-

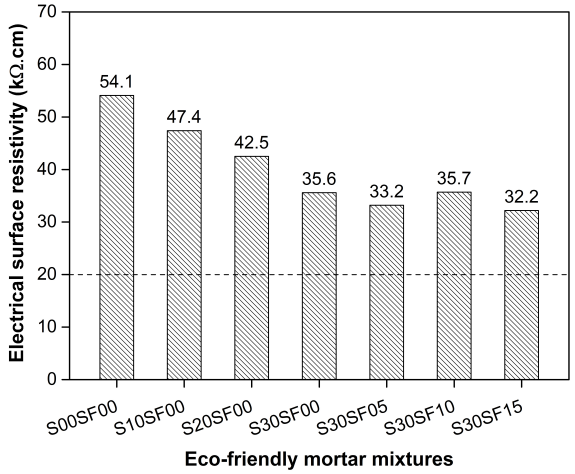

Fig. 8. ESR of the eco-friendly mortar samples.

strating its effectiveness as a barrier [47].

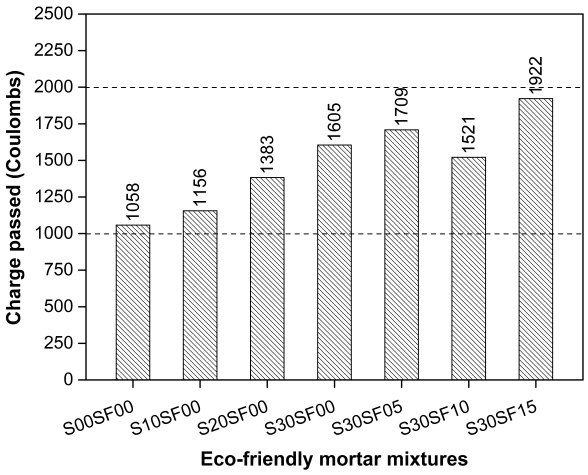

Fig. 9. RCP of the eco-friendly mortar samples.

4.6. Thermal conductivity

The TC values recorded for the eco-friendly marine mortar samples under both SSD and OD conditions are shown in Fig. 10. The trend for TC was similar to that for ESR. The TC values of the samples under the SSD condition declined from 1.548 W/mK to 1.348 W/mK, while those under the OD condition, with the exception of S30SF10, declined from 1.429 W/mK to 1.125 W/mK. The OD mortar samples earned TC values that were around 8.3 – 19.8% below those of the SSD mortar samples. This difference in TC at different sample conditions was reported previously by Hwang and Tran [45]. On the other hand, a close relationship between TC and porosity was found, as higher porosity was associated with lower TC [45]. As observed in the SEM morphologies of the eco-friendly mortar samples (Fig. 11), the increase in pore/void structures with increasing GGBFS content was associated with a reduction in TC values. This explanation also holds true for the mortar samples with various levels of SF content. Its more-solid structure earned S30SF10 (Fig. 12c) a higher TC value than the other samples in the SF group.

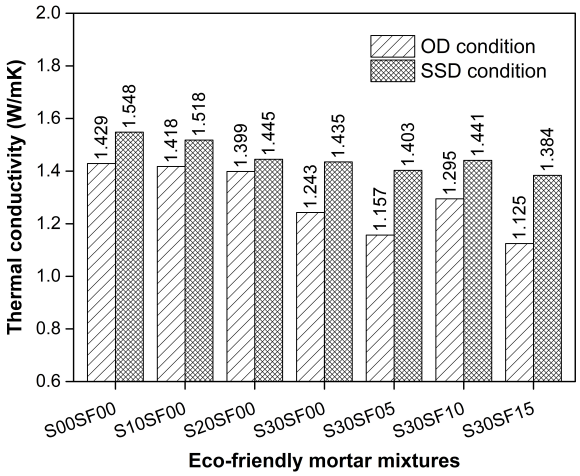

Fig. 10. TC of the eco-friendly mortar samples.

4.7. Microstructure analysis

The microstructures of the eco-friendly mortar samples are shown in Figs. 11 and 12, with the SEM micrographs of S00SF00, S10SF00, S20SF00, and S30SF00 shown in Fig. 11 and those of S30SF00, S30SF05, S30SF10, and S30SF15 shown in Fig. 12. Microcracking, primarily due to the compression test, as mentioned in the previous section, was observed in most of the SEM micrographs of the samples. Moreover, more microcracking and less-dense microstructures were observed in the SEM images of the mortar samples with higher GGBFS contents. The fracture patterns were propagated in the S20SF00 sample (Fig. 11c). Furthermore, a hole was generated in the S30SF00 sample (Fig. 11d).

On the other hand, the samples with higher SF contents exhibited relatively denser microstructures, leading to higher strength and lower RCP, as mentioned previously in this study (see Figs. 4, 5, 9).

5. Conclusions

This study was designed to examine the feasibility of using ternary mixtures of cementitious additives, including GGBFS, FA, and SF, to produce eco-friendly mortars applicable in general construction and, particularly, in the repair and maintenance of corroded concrete structures. The engineering properties and durability of the proposed

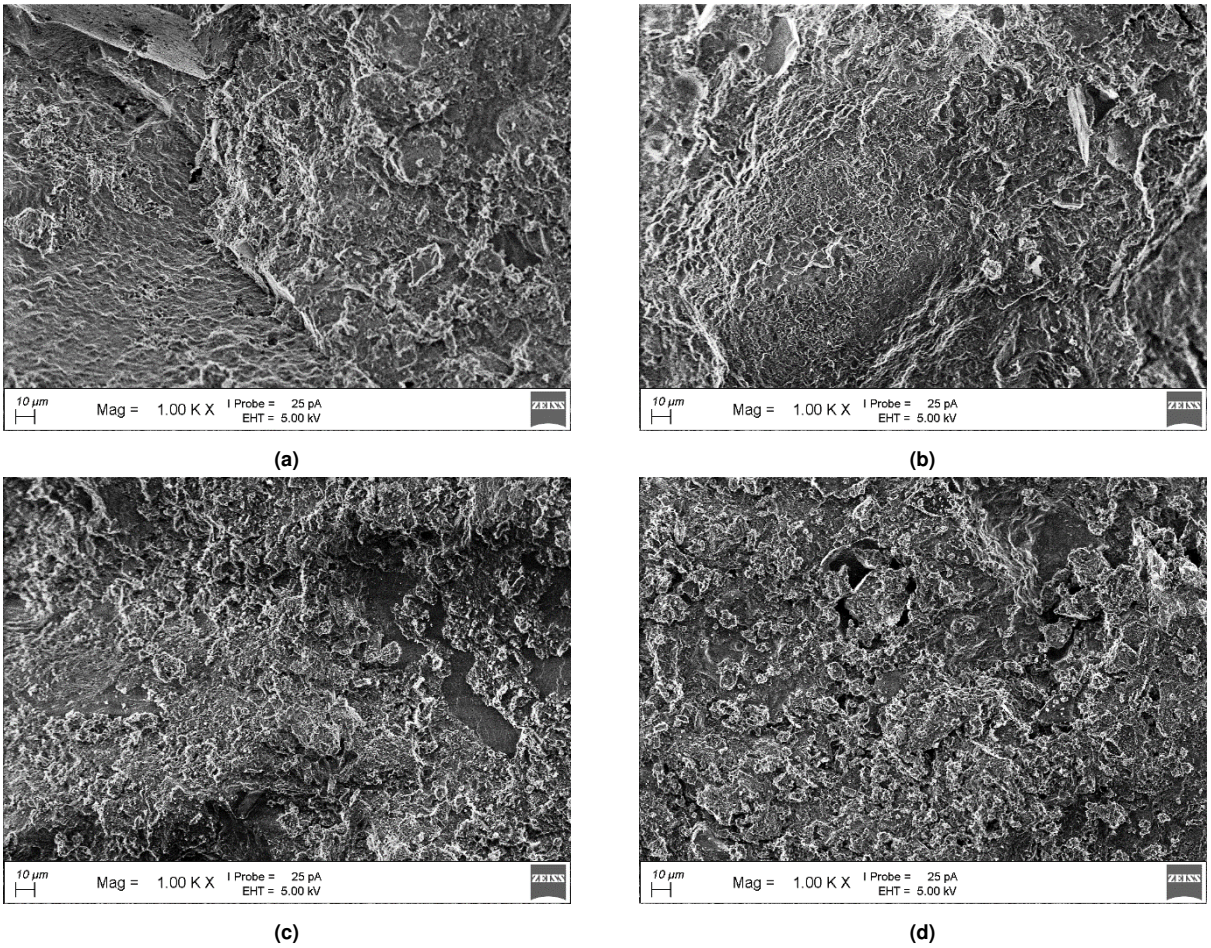

Fig. 11. SEM micrographs of the eco-friendly mortar samples with various GGBFS contents: (a) S00SF00, (b) S10SF00, (c) S20SF00, and (d) S30SF00.

mortar samples were examined and discussed. The following conclusions may be made based on the experimental outcomes:

1) In general, replacing cement with GGBFS reduced the compressive and flexural strengths of the samples. At 56 days of curing age, the compressive and flexural strength values were 48.5 MPa and 10.5 MPa, respectively, for the 30% GGBFS specimens. Moreover, the highest 56-day compressive and flexural strength values for the 10% SF specimens were 49.2 MPa and 13.8 MPa, respectively. Thus, adding silica fume may be considered as an effective approach to improving mortar strength. However, an excess amount of SF may cause a reduction in the compressive strength of the mortars.

2) Lower UPV values were found at the eco-friendly mortar with higher GGBFS replacement levels and the incorporation of 10% SF slightly increased the UPV values of the mortar samples. However, the UPV values of the mortar samples in this study ranged from 4038 to 4158 m/s (>3660 m/s), indicating that all were "high-quality" mortars under the definition proposed by Malhotra (1976).

3) Increasing the amount of GGBFS reduced ESR in the mortar samples, with S00SF00, S10SF00, S20SF00, and S30SF00 earning ESR values of 54.1, 47.4, 42.5, and 35.6 kΩ.cm, respectively. Besides, the ESR values were 35.6, 33.2, 35.7, and 32.2 kΩ.cm for the mortar samples with 0, 5, 10, and 10% SF, respectively. A similar trend was found for the TC measurement of the mortar samples. Thus, the results of the ESR and TC tests further supported an optimum mixture containing 30% GGBFS and 10% SF. The internal structure of the mixture impacted the heat transfer and the charge on the surface, with this impact enhanced by the increase in both additives (GGBFS and SF).

4) In terms of RCP, the total charge transferred through the mortar samples was positively associated with the level of GGBFS replacement in the mortar mixtures and the mortar samples containing 10% SF exhibited better chloride permeability resistance than the mortar samples with 0%,

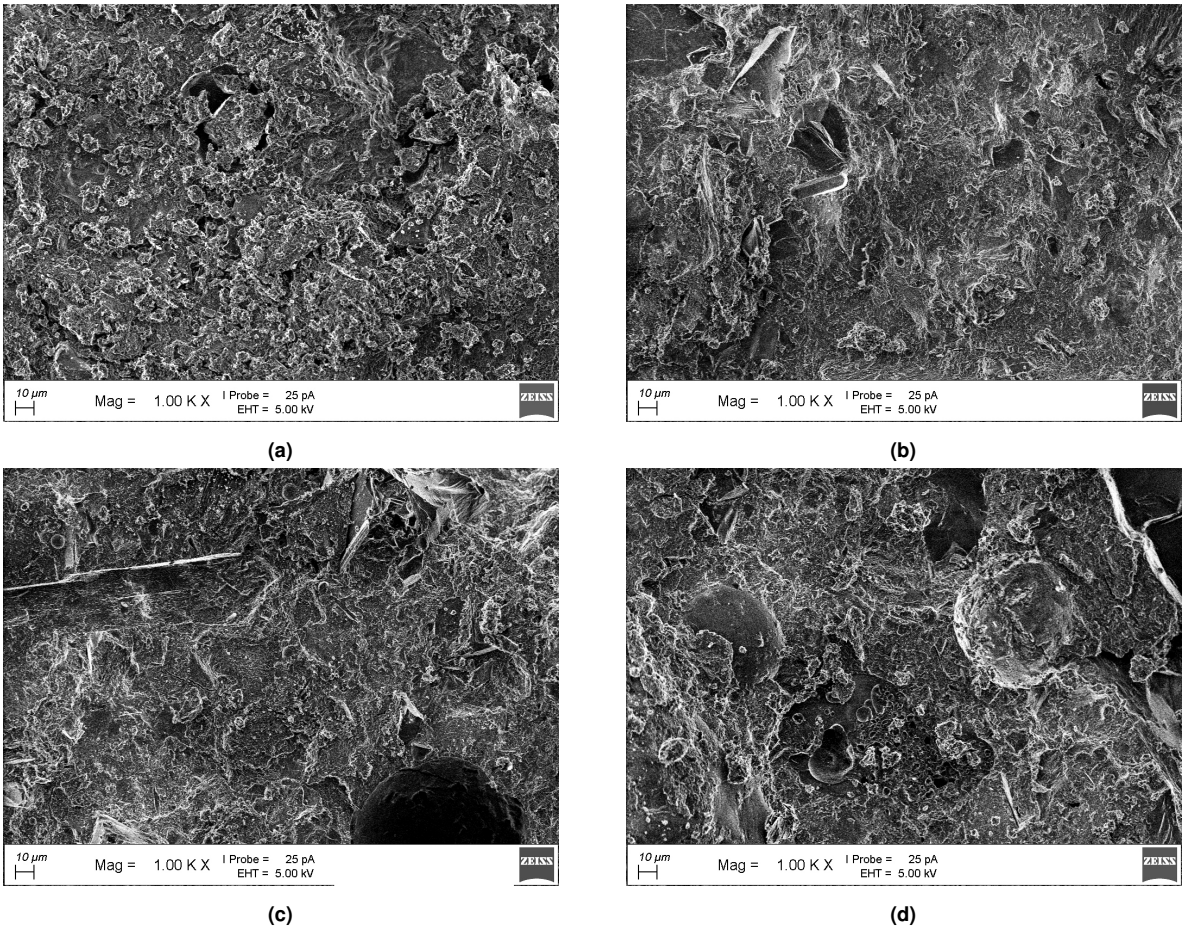

Fig. 12. SEM micrographs of the eco-friendly mortar samples with various SF contents: (a) S30SF00, (b) S30SF05, (c) S30SF10, and (d) S30SF15.

5%, and 15% SF. As a result, the total charge that passed through the mortar samples ranged between 1058 and 1922 Coulombs, demonstrating that all of the specimens had low chloride-ion permeability and good corrosion resistance, especially in chloride-contaminated environments.

5) Although the incorporation of locally available and sourced GGBFS and SF was not found to significantly improve the engineering performance of the mortar samples, based on the experimental results, the proposed eco-friendly mortars exhibited good mechanical and durability performance. The incorporation of industrial by-products may be expected to bring benefits in terms of reducing landfill loading and improving the environmental sustainability of the construction industry.

References

[1] P Novak, AIB Moffat, C Nalluri, and R Narayanan. Hydraulic Structures: Fourth Edition. 2007.

[2] Zhongru Wu, Ji Li, Chongshi Gu, and Huaizhi Su. Review on hidden trouble detection and health diagnosis of hydraulic concrete structures. *Science in China, Series E: Technological Sciences*, 50:34–50, 2007.

[3] Yi Li, Mingyue Wan, Jiming Du, Li Lin, Wei Cai, and Longfei Wang. Microbial enhanced corrosion of hydraulic concrete structures under hydrodynamic conditions: Microbial community composition and functional prediction. *Construction and Building Materials*, 248, 2020.

[4] Yarong Song, Yimei Tian, Xuan Li, Jing Wei, Haiya Zhang, Philip L. Bond, Zhiguo Yuan, and Guangming Jiang. Distinct microbially induced concrete corrosion at the tidal region of reinforced concrete sewers. *Water Research*, 150:392–402, 2019.

[5] Julia A. Maresca, Paul Moser, and Thomas Schumacher. Analysis of bacterial communities in and on concrete. *Materials and Structures*, 50(1), 2017.

[6] P. Kumar Mehta and Richard W. Burrows. Building durable structures in the 21st century. *Indian Concrete*

Journal, 75(7):437–443, 2001.

[7] R. S. Olivito, O. A. Cevallos, and A. Carrozzini. Development of durable cementitious composites using sisal and flax fabrics for reinforcement of masonry structures. *Materials and Design*, 57:258–268, 2014.

[8] Jahangir Mirza, Benoit Durand, Aamer R. Bhutta, and Mahmood M. Tahir. Preferred test methods to select suitable surface repair materials in severe climates. *Construction and Building Materials*, 50:692–698, 2014.

[9] Romy S Edwin, Mieke De Schepper, Elke Gruyaert, and Nele De Belie. Effect of secondary copper slag as cementitious material in ultra-high performance mortar. *Construction and Building Materials*, 119:31–44, 2016.

[10] Jixiang Wang, Tianyong Huang, Guodong Cheng, Ze Liu, Siqi Li, and Dongmin Wang. Effects of fly ash on the properties and microstructure of alkali-activated FA/BFS repairing mortar. *Fuel*, 256, 2019.

[11] Rafael Robayo-Salazar, Carlos Jesús, Ruby Mejía de Gutiérrez, and F. Pacheco-Torgal. Alkali-activated binary mortar based on natural volcanic pozzolan for repair applications. *Journal of Building Engineering*, 25, 2019.

[12] Hui Zhao, Wei Sun, Xiaoming Wu, and Bo Gao. The properties of the self-compacting concrete with fly ash and ground granulated blast furnace slag mineral admixtures. *Journal of Cleaner Production*, 95:66–74, 2015.

[13] Erdoan Özbay, Mustafa Erdemir, and Halil Ibrahim Durmuş. Utilization and efficiency of ground granulated blast furnace slag on concrete properties - A review. *Construction and Building Materials*, 105:423–434, 2016.

[14] Trong Phuoc Huynh, Duy Hai Vo, and Chao Lung Hwang. Engineering and durability properties of eco-friendly mortar using cement-free SRF binder. *Construction and Building Materials*, 160:145–155, 2018.

[15] Chao Lung Hwang, Duy Hai Vo, and Trong Phuoc Huynh. Physical–microstructural evaluation and sulfate resistance of no-cement mortar developed from a ternary binder of industrial by-products. *Environmental Progress and Sustainable Energy*, 39(5), 2020.

[16] Li Jianyong and Tian Pei. Effect of slag and silica fume on mechanical properties of high strength concrete. *Cement and Concrete Research*, 27(6):833–837, 1997.

[17] Svetlana Pushkar. The effect of additional byproducts on the environmental impact of the production stage of concretes containing bottom ash instead of sand. *Sustainability*, 11(18), 2019.

[18] TCVN10302:2014. Activity admixture - Fly ash for concrete, mortar and cement. *Ministry of Science and Technology, Vietnam. (in Vietnamese)*, 2014.

[19] ASTMC618. Standard specification for coal fly ash and raw or calcined natural pozzolan for use in concrete. *ASTM International, West Conshohocken, PA*, 2019.

[20] Ana Fernández-Jiménez and A Palomo. Mid-infrared spectroscopic studies of alkali-activated fly ash structure. *Microporous and mesoporous materials*, 86(1-3):207–214, 2005.

[21] Ghasan Fahim Huseien, Abdul Rahman Mohd Sam, Kwok Wei Shah, Mohammad Ali Asaad, Mahmood Md Tahir, and Jahangir Mirza. Properties of ceramic tile waste based alkali-activated mortars incorporating GBFS and fly ash. *Construction and Building Materials*, 214:355–368, 2019.

[22] TCVN3121–2:2003. Mortar for masonry - Test methods Part 2: Sampling and preparation of specimens. *Ministry of Science and Technology, Vietnam. (in Vietnamese)*, 2003.

[23] ASTM109. Standard test method for compressive strength of hydraulic cement mortars (using 2 in. or [50 mm] cube specimens). *ASTM International, West Conshohocken, PA*, 2020.

[24] TCVN3121–11:2003. Mortar for masonry - Test methods Part 11: Determination of flexural and compressive strength of hardened mortars. *Ministry of Science and Technology, Vietnam. (in Vietnamese)*, 2003.

[25] ASTMC597. Standard test method for pulse velocity through concrete. *ASTM International, West Conshohocken, PA*, 2016.

[26] ASTMC1202. Standard test method for electrical indication of concrete's ability to resist chloride ion penetration. *ASTM International, West Conshohocken, PA*, 2019.

[27] Richard J Kessler, Rodney G Powers, and M A Paredes. Resistivity measurements of water saturated concrete as an indicator of permeability. *Proceedings of the Corrosion*, 2005.

[28] Chao Lung Hwang, Le Anh Tuan Bui, Kae Long Lin, and Chun Ting Lo. Manufacture and performance of lightweight aggregate from municipal solid waste incinerator fly ash and reservoir sediment for self-consolidating lightweight concrete. *Cement and Concrete Composites*, 34(10):1159–1166, 2012.

[29] M Schneider, M Romer, M Tschudin, and H. Bolio. Sustainable cement production-present and future. *Cement and Concrete Research*, 41(7):642–650, 2011.

[30] Idawati Ismail, Susan A. Bernal, John L. Provis, Rackel San Nicolas, Sinin Hamdan, and Jannie S.J. Van Deventer. Modification of phase evolution in alkali-activated blast furnace slag by the incorporation of fly ash. *Cement and Concrete Composites*, 45:125–135, 2014.

[31] Watcharapong Wongkeo, Pailyn Thongsanitgarn, Athipong Ngamjarurojana, and Arnon Chaipanich. Compressive strength and chloride resistance of self-compacting concrete containing high level fly ash and silica fume. *Materials and Design*, 64:261–269, 2014.

[32] Sinan Caliskan. Aggregate/mortar interface: Influence of silica fume at the micro- and macro-level. *Cement and Concrete Composites*, 25(4-5 SPEC):557–564, 2003.

[33] N. Bouzoubaâ, M. H. Zhang, and V. M. Malhotra. Mechanical properties and durability of concrete made with high-volume fly ash blended cements using a coarse fly ash. *Cement and Concrete Research*, 31(10):1393–1402, 2001.

[34] Arnon Chaipanich, Rattiyakorn Rianyoi, and Thanongsak Nochaiya. The effect of carbon nanotubes and silica fume on compressive strength and flexural strength of cement mortars. *Materials Today: Proceedings*, 4(5):6065–6071, 2017.

[35] S Bhanja and B Sengupta. Influence of silica fume on the tensile strength of concrete. *Cement and concrete research*, 35(4):743–747, 2005.

[36] Xiaoying Xu, Xujian Lin, Xiaoxin Pan, Tao Ji, Yongning Liang, and Hongru Zhang. Influence of silica fume on the setting time and mechanical properties of a new magnesium phosphate cement. *Construction and Building Materials*, 235, 2020.

[37] Zemei Wu, Caijun Shi, and K H Khayat. Influence of silica fume content on microstructure development and bond to steel fiber in ultra-high strength cement-based materials (UHSC). *Cement and Concrete Composites*, 71:97–109, 2016.

[38] Mouhcine Benaicha, Xavier Roguiez, Olivier Jalbaud, Yves Burtschell, and Adil Hafidi Alaoui. Influence of silica fume and viscosity modifying agent on the mechanical and rheological behavior of self compacting concrete. *Construction and Building Materials*, 84:103–110, 2015.

[39] Mahdi Valipour, Farhad Pargar, Mohammad Shekarchi, and Sara Khani. Comparing a natural pozzolan, zeolite, to metakaolin and silica fume in terms of their effect on the durability characteristics of concrete: A laboratory study. *Construction and Building Materials*, 41:879–888, 2013.

[40] N Flores Medina, G Barluenga, and Francisco Hernández-Olivares. Combined effect of polypropylene fibers and silica fume to improve the durability of concrete with natural pozzolans blended cement. *Construction and Building Materials*, 96:556–566, 2015.

[41] Punnaman Norrarat, Weerachart Tangchirapat, Smith Songpiriyakij, and Chai Jaturapitakkul. Evaluation of Strengths from Cement Hydration and Slag Reaction of Mortars Containing High Volume of Ground River Sand and GGBF Slag. *Advances in Civil Engineering*, 2019, 2019.

[42] V. M. Malhotra. Testing hardened concrete: Nondestructive methods. *ACI Monograph No. 9, ACI. Iowa State University Press, Ames, Iowa.*, 1976.

[43] Zoubeir Lafhaj, Marc Goueygou, Assia Djerbi, and Mariusz Kaczmarek. Correlation between porosity, permeability and ultrasonic parameters of mortar with variable water / cement ratio and water content. *Cement and Concrete Research*, 36(4):625–633, 2006.

[44] Pejman Azarsa and Rishi Gupta. Electrical Resistivity of Concrete for Durability Evaluation: A Review. *Advances in Materials Science and Engineering*, 2017, 2017.

[45] Chao-Lung Hwang and Vu-An Tran. Engineering and Durability Properties of Self-Consolidating Concrete Incorporating Foamed Lightweight Aggregate. *Journal of Materials in Civil Engineering*, 28(9):04016075, 2016.

[46] ASTMC1202. Standard test method for electrical indication of concrete's ability to resist chloride ion penetration. *ASTM International, West Conshohocken, PA.*, 2019.

[47] Xuemei Liu, Kok Seng Chia, and Min Hong Zhang. Water absorption, permeability, and resistance to chloride-ion penetration of lightweight aggregate concrete. *Construction and Building Materials*, 25(1):335–343, 2011.